2022 EAGE ANNUAL
83RD CONFERENCE & EXHIBITION
MADRID I SPAIN

A SEMI-ANALYTICAL MODEL FOR THE PREDICTION OF CO2 INJECTIVITY INTO SALINE AQUIFERS OR DEPLETED HYDROCARBON RESERVOIRS

T. Whittle[1]*, P. Park[1], C. Coll[1]

[1] CGG

Full SPE Paper Title

A Semi-Analytical Model for the Prediction of CO2 Injectivity into Saline Aquifers or Depleted Hydrocarbon Reservoirs

Society of Petroleum Engineers

SPE-209628-MS

A Semi-Analytical Model for the Prediction of CO2 Injectivity into Saline Aquifers or Depleted Hydrocarbon Reservoirs

Tim Whittle, Philippa Park, and Carolina Coll, CGG

 DOI 10.2118/209628-MS

This paper was prepared for presentation at the SPE EuropEC - Europe Energy Conference featured at the 83rd EAGE Annual Conference & Exhibition held in Madrid, Spain, 6 - 9 June 2022.

Abstract

As carbon dioxide (CO_2) is injected into a reservoir (for CO_2 sequestration in a saline aquifer or depleted reservoir, or even for enhanced oil recovery in the case of a less depleted reservoir), a region around the well becomes saturated and expands with time. From a pressure transient perspective, by making some simple assumptions the resulting reservoir configuration at any given moment can be approximated by a two-region radial composite system. As well as its radial extent, the inner region is defined by its diffusivity and mobility, both of which differ from those of the outer region as a result of the CO_2 saturation. The CO_2 viscosity and compressibility at reservoir pressure and temperature are the essential properties that impact the diffusivity and mobility. Knowing the three variables, radius, diffusivity ratio and mobility ratio, the constant rate pressure transient response is readily computed from existing analytical radial composite model solutions. These are commonly used in the petroleum industry to analyse well test behaviour and can be configured with a variety of boundary conditions (no flow, constant pressure or infinite, usually in the shape of a rectangle).

The problem with CO_2 injection is that the radius and properties of the inner zone vary with time and hence any single radial composite model does not apply. The solution approach in this paper is to apply superposition. At each discretised time step, the well is simultaneously injected at a constant rate assuming the current configuration and shut in with the previous configuration. The shut-in "cancels out" the previous model and the current model applies. At each time step, the injected volume is calculated, the material balance and associated reservoir pressure computed along with the new inner zone radius, diffusivity and mobility and hence the model for the next time step is defined. An additional iterative loop allows for the injection rate to decrease if the injection pressure exceeds a maximum constraint.

The method is simple and fast and appears to match the pressure response of numerical simulations of the same problem using more detailed physics, without the associated noisy derivative often associated with grid-based solutions. It implicitly assumes a piston like displacement which results in an unrealistic saturation profile that differs from the more rigorous numerical models where gravity and capillary effects are included. However, comparisons with such models indicate that the prediction of well pressure and hence injectivity is sufficiently accurate for practical purposes despite this approximation.

The application of superposition in time - a method usually associated with solving linear problems – is demonstrated to adequately solve the complex non-linear problem of CO_2 injectivity and, because the method includes material balance, it can help to define storage efficiency factors which are critical for the evaluation of storage capacity.

Introduction

The motivation for this study was to develop a simple solution that relies on minimum information and yet provides predictions of CO_2 injectivity in a variety of scenarios with sufficient accuracy to, for example, facilitate the storage screening of best candidate depleted reservoirs or aquifers for CO_2 sequestration.

Several authors have studied the problem of injectivity of carbon dioxide into subsurface porous media - Law & Bachu (1996), Nordbotten et al (2005), Burton et al (2008), Ehlig-Economides & Economides (2009), Mathias et al (2010), Peysson et al (2013), Ringrose & Meckel (2019). Each assume varying degrees of complexity and approximation, but none have applied the method proposed in this paper.

Kamal et al (2019) solved a similar problem for Polymer flooding by deriving a complex but fully analytical solution. It was shown to accurately simulate pressure fall-offs after injection but they did not demonstrate how well it worked for the injection period itself.

The assumptions and theory behind our method are discussed and examples presented and compared with numerical models that consider the physics more rigorously. Advantages and limitations are highlighted, and conclusions drawn including recommendations for future study.

In the petroleum industry, the pressure transient analysis of well tests is a routine process that relies on a variety of software applications that allow analytical and numerical modelling of the observed pressure response to a given set of measured rates. Analytical models are useful because they are simple and rely on a minimum amount of information but are only valid if the solution to the diffusivity equation that describes fluid flow can be assumed to be linear. Several data transformations (e.g. pseudo-pressure for gas) are made to try to linearize what may otherwise be a non-linear problem. In the case of the injection of carbon dioxide into either a saline aquifer or a depleted hydrocarbon reservoir, a significant source of non-linearity is the two-phase nature of the problem. CO2 in carbon sequestration projects is typically injected as a supercritical fluid due to the operational advantages that this has for transporting offshore.

A Homogeneous Reservoir Model

Before CO_2 is injected, the reservoir is assumed to contain water, oil and or hydrocarbon gas at a uniform static pressure (p_i) with each phase at a constant saturation (S_w, S_o and S_g) and compressibility (c_w, c_o, and c_g). There is only one mobile phase with viscosity (μ) which, in the case of water or oil is assumed constant but in the case of gas, varies with pressure. The reservoir is homogeneous with a uniform thickness (h), constant permeability (k), porosity (ϕ) and total compressibility (c_t):

$$c_t = S_o c_o + S_g c_g + S_w c_w + c_f \tag{1}$$

with formation compressibility (c_f) also constant.

The reservoir can be bounded on four sides in the form of a rectangle of a given area ($A = X_e \times Y_e$) with each boundary being either no-flow, constant pressure or infinite. The well with a radius, r_w, is located at coordinates (X_w, Yw) from the origin of the rectangle and has constant wellbore storage, C, and skin, S, With this configuration, analytical solutions to the bottomhole pressure response versus time ($\Delta p(\Delta t) = |p_i - p(\Delta t)|$) of a well flowing (or injecting) at constant surface rate, q, may be expressed in dimensionless terms thus:

$$p_D = f\left(t_D, C_D, S, A_D, \frac{X_e}{Y_e}, \frac{X_w}{X_e}, \frac{Y_w}{Y_e}\right) \tag{2}$$

Where in consistent units and with the surface rate, q, converted to downhole rate with the formation volume factor, B:

$$p_D = 2\pi \frac{kh}{qB\mu} \Delta p \tag{3}$$

$$t_D = \frac{k}{\phi \mu c_t r_w^2} \Delta t \tag{4}$$

$$C_D = \frac{C}{2\pi \phi c_t h r_w^2} \tag{5}$$

$$A_D = \frac{A}{r_w^2} \tag{6}$$

For infinite boundary conditions, the function, f, is typically derived in Laplace space (Agarwal et al -1970) and then inverted numerically (Stehfest -1970). For bounded systems a Green's functions approach is more appropriate (Gringarten & Ramey – 1973).

Because the CO_2 to be injected is not the same fluid as contained in the reservoir, this model does not apply. The CO_2 will develop a zone around the well of different fluid viscosity and compressibility to that of the surrounding reservoir. At any given time, assuming a piston like displacement with no solubility and ignoring gravity, the CO_2 will form a circular zone around the well as illustrated in Figure 1.

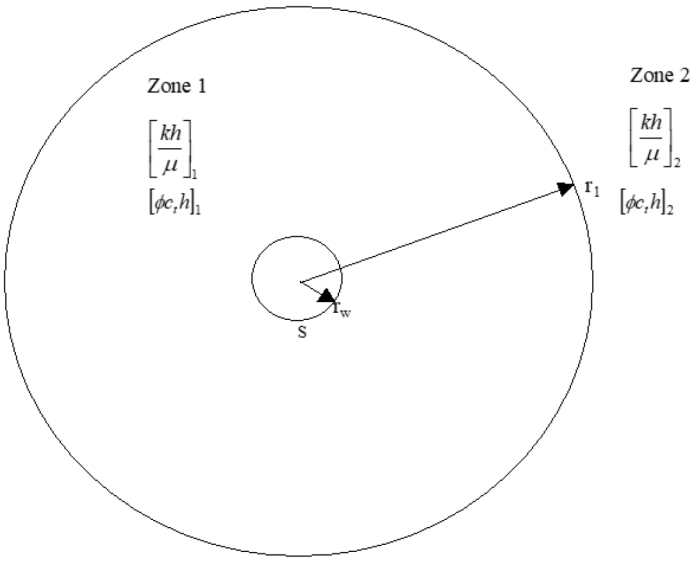

Figure 1—Radial Composite Reservoir Model

A Radial Composite Model

The radial composite model assumes two zones, an inner zone 1 of radius, r_1, with mobility thickness, $\left[\frac{kh}{\mu}\right]_1$ and storativity, $[\phi c_t h]_1$, surrounded by the outer reservoir zone 2. Dimensionless pressure, p_D, time, t_D, and wellbore storage coefficient, C_D, are all based on zone 1 and three additional dimensionless parameters define the model:

$$r_{1D} = \frac{r_1}{r_w} \tag{7}$$

$$\kappa = \frac{\left[\frac{kh}{\mu}\right]_1}{\left[\frac{kh}{\mu}\right]_2} \tag{8}$$

$$\omega = \frac{[\phi c_t h]_1}{[\phi c_t h]_2} \tag{9}$$

Combined with the boundary effects described above for the homogeneous model, the pressure transient response of a well in a radial composite rectangular reservoir may be expressed:

$$p_{D1} = g\left(t_{D1}, C_{D1}, S, r_{1D}, \kappa, \omega, A_D, \frac{X_e}{Y_e}, \frac{X_w}{X_e}, \frac{Y_w}{Y_e}\right) \tag{10}$$

For infinite boundary conditions, and circular reservoirs, the function g, is solved in Laplace space (Kikani & Walkup – 1991) and an example infinite acting response on a log-log plot of pressure change and derivative versus time (Bourdet et al – 1983, 1989) is illustrated in Figure 2.

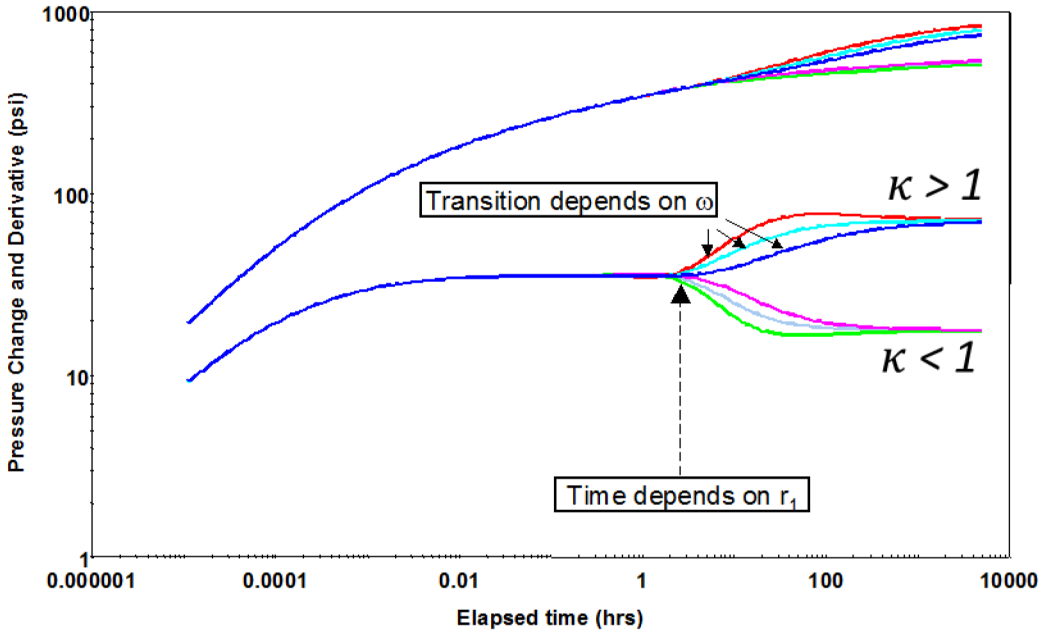

Figure 2—Log-log plot of a variety of radial composite model pressure transient responses

For rectangular reservoirs used in this study, the bounded system response minus the infinite acting response of a homogeneous reservoir is added to the infinite acting response of the radial composite reservoir. Provided that the inner zone radius is not too large compared to the distance to the reservoir boundaries, this superposition is a good approximation. However, a correction to the dimensionless reservoir area must be made to maintain material balance. At constant rate, the average pressure change according to pseudo-steady state material balance is:

$$\Delta\overline{p} = \frac{qB\Delta t}{[\,\emptyset\, c_t h A]_T} \tag{11}$$

Where:

$$[\,\emptyset\, c_t h A]_T = [\,\emptyset\, c_t h A]_1 + [\,\emptyset\, c_t h A]_2 \tag{12}$$

A_1 is the area of the inner zone (including the well):

$$A_1 = \pi r_1^2 \tag{13}$$

And A_2 is the area of the outer zone:

$$A_2 = A - A_1 \tag{14}$$

Hence:

$$[\emptyset c_t hA]_T = [\emptyset c_t h]_1 \pi r_1^2 + [\emptyset c_t h]_2 \left(A - \pi r_1^2\right) \tag{15}$$

Converting Equation (11) into dimensionless pressure per Equation (3):

$$\bar{p}_D = \frac{2\pi}{qB}\left[\frac{kh}{\mu}\right]_1 \frac{qB\Delta t}{[\emptyset c_t hA]_T} \tag{16}$$

And dimensionless time using Equation (4):

$$\bar{p}_D = 2\pi t_D \frac{[\emptyset c_t h]_1}{[\emptyset c_t h]_1 \pi r_1^2 + [\emptyset c_t h]_2 \left(A - \pi r_1^2\right)} r_w^2 \tag{17}$$

which simplifies to:

$$\bar{p}_D = 2\pi t_D \frac{1}{\pi r_{1D}^2 + \frac{1}{\omega}\left(A_D - \pi r_{1D}^2\right)} \tag{18}$$

Thus, before the superposition, the homogeneous closed system response is adjusted by replacing A_D with a modified dimensionless reservoir area A_D' defined:

$$A_D' = \pi r_{1D}^2 + \frac{1}{\omega}\left(A_D - \pi r_{1D}^2\right) \tag{19}$$

Note that when $\omega = 1$, $A_D' = A_D$. To calculate the actual pressure change at a given time, two additional parameters are required: Pressure Match, PM, and Time Match, TM, which are defined by Equations (3) and (4) based on the inner zone 1 parameters:

$$PM = \frac{p_{D1}}{\Delta p} = 2\pi \frac{1}{qB}\left[\frac{kh}{\mu}\right]_1 \tag{20}$$

$$TM = \frac{t_{D1}}{\Delta t} = \frac{1}{r_w^2}\left[\frac{kh}{\mu}\right]_1 \frac{1}{[\phi c_t h]_1} \tag{21}$$

Hence, at a given time, Δt, following injection at a constant rate, q, into a radial composite reservoir with rectangular boundaries, the pressure change, $\Delta p(\Delta t)$, at the well is calculated as follows:

$$\Delta p(\Delta t) = \frac{1}{PM} g\left(\Delta t \times TM, C_{D1}, S, r_{1D}, \kappa, \omega, A_D', \frac{X_e}{Y_e}, \frac{X_w}{X_e}, \frac{Y_w}{Y_e}\right) \tag{22}$$

Non-Linearity: Multi-model superposition

The problem remains that as injection proceeds, the radius of the inner zone increases with time and as the pressure increases the fluid properties change. The analytical solution to the radial composite model cannot include these non-linearities. The proposed solution to this problem is again to apply superposition. As with numerical models, the analytical solution is typically computed at discrete times that increase logarithmically up to maximum timestep. In this case, at each timestep, following the computation of the pressure change with the current model, the well is shut-in and then simultaneously opened assuming an updated model that includes the change in the reservoir configuration. A shut-in is another form of superposition where the well is initially flowed at a given rate and then simultaneously flowed at an equal and opposite rate starting from the time of shut in.

Following the first timestep, the well pressure, *p(t)*, (Figure 3) is calculated from three distinct responses corresponding to two models, A and B, which in this case are both radial composite but with differing parameters. Figure 3 depicts the three pressure responses, (1), (2) and (3) and the resulting calculation of *p(t)* is the initial pressure, p_i plus:

1. the pressure change due to constant rate injection starting from time zero according to Model A, minus
2. the pressure change due to constant rate production starting from time t_1 according to Model A, plus
3. the pressure change due to constant rate injection starting from time t_1 according to Model B.

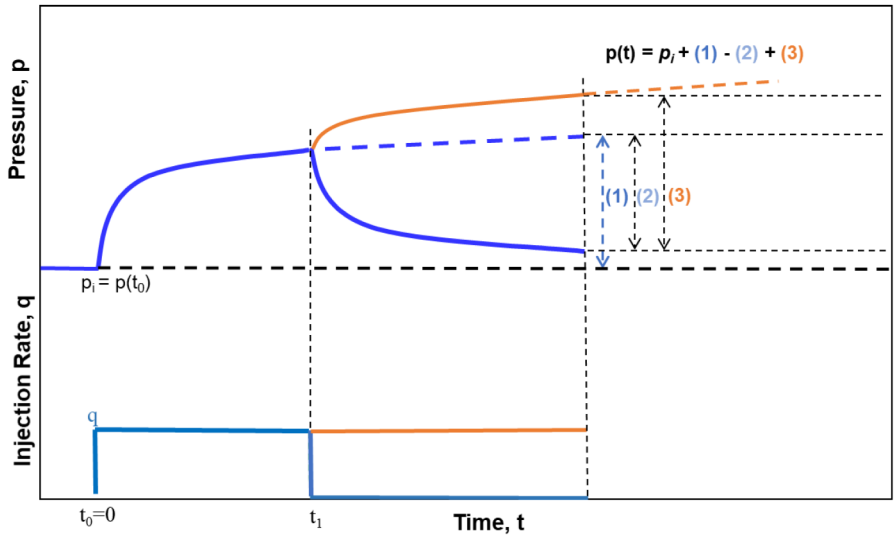

Figure 3—Schematic of Changing Model Superposition

This method is propagated and repeated for each step at which a new set of model parameters (model C, D… etc) are calculated along with the associated model responses. The method is general for any change in model versus time but in this case of CO_2 injection, the model remains radial composite and it is only the model parameters and the response which change.

Model Parameters that Change with CO_2 Injection

As the injection of CO_2 proceeds, at each timestep, various parameters must be recalculated. In the case of a closed reservoir, the average reservoir pressure, $\bar{p}$ increases with cumulative injection. This results in a change in fluid properties. Isothermal conditions are assumed and hence it is sufficient to have a table of fluid properties versus pressure from which a table lookup algorithm can provide a particular property at any given pressure. The properties versus pressure of CO_2 are complex because it can change phase or become supercritical. The table of properties (formation volume factor, density, compressibility and viscosity) must take this into account. Around the well, it is quite likely that the temperature is not constant during injection. Further away, it is expected that the temperature will stabilise to that of the surrounding reservoir. The impact of temperature changes has not been considered in this work and should probably be studied further.

Rock compressibility, c_r, is assumed constant but this implies an increase of porosity with pressure:

$$\phi(\bar{p}) = \phi(p_i)e^{(c_r(\bar{p}-p_i))} \tag{23}$$

The cumulative volume of CO_2 injected at any timestep, V_g, occupies a volume in the reservoir according the gas formation volume factor B_g at the average reservoir pressure:

$$V_g = B_g(\bar{p})qt \tag{24}$$

From this volume and assuming an irreducible water saturation, S_{wi}, the radius of the inner zone, r_1, is known:

$$r_1 = \sqrt{\frac{V_g}{\pi\phi(\bar{p})h(1-S_{wi})}} \tag{25}$$

Assuming a saline aquifer, the reservoir is initially fully saturated with water of volume, V_w, equal to the reservoir pore volume:

$$V_w = \phi Ah \tag{26}$$

As CO_2 is injected the water is displaced and its volume reduces but at the same time, as the pressure increases, the porosity increases. So, the change in water volume, δV_w, is equal to the volume of gas injected minus the increase in pore volume:

$$\delta V_w = V_g - \phi(p_i)\left[e^{(c_r(\overline{p}-p_i))}-1\right] \tag{27}$$

The change in water volume results in a change in average pressure, $\delta\overline{p}$, dependent on the water compressibility:

$$\delta\overline{p} = \frac{\delta V_w}{V_w}\frac{1}{c_w} \tag{28}$$

And hence a change in average pressure:

$$\overline{p} = p_i + \delta\overline{p} \tag{29}$$

This leads to an iterative calculation of $\overline{p}$ that satisfies both Equations (24) & (29). In practice, water compressibility varies slightly with pressure which complicates the calculation, but the same principle applies. A similar approach is also taken in the case of injecting CO_2 into a reservoir containing oil or gas.

Once a consistent average pressure is obtained, the other pressure dependent fluid properties (viscosity and compressibility) are calculated along with the corresponding model parameters $(PM, TM, C_{D1}, r_{1D}, \kappa, \omega, A_D')$ ready for the next timestep and the new response is computed.

Compared to a single instance of the same analytical model, computation times for this multi-model semi-analytical method increase by the square of the number of timesteps. For each of the test examples considered in this paper, using a VBA implementation in Excel on a laptop computer (64-bit Windows 10, Intel i7 2.6 GHz, 16Gb Ram), the calculations took less than ten seconds.

Example 1 Closed Saline Aquifer

The assumed well and reservoir properties for this example case are listed in Table 1. The relevant CO_2 and water fluid properties as a function pressure are listed in Table 2 (in the calculations, smaller pressure intervals were used). A well placed in the center of the reservoir is assumed to inject CO_2 at a maximum rate of 1MMscf/d (0.0189 MT/year) for ten years followed by a 2500 hr shut-in for a pressure build-up. Two examples are considered: Example 1a is run with unconstrained pressure whilst Example 1b is constrained to a maximum pressure of 7000 psia.

Table 1—Input Data for Example 1 and 2

Example 1 &2 Input Data			
Parameter	**unit**	**value**	
Reservoir Properties		**Example 1**	**Example 2**
Permeability, k	md	33.333	33.333
Thickness, h	ft	30	30
Porosity, ϕ		0.1	0.1
Rock Compressibility, c_r	1/psi	3.00E-06	3.00E-06
Irreducible Water Saturation, S_{wi}		0.1	n/a
Residual Oil Saturation, S_{or}		n/a	0.1
Initial Reservoir pressure, p_i	psi	5000	2000
Reservoir Temperature, T_{res}	°F	212	212
Water Viscosity at Tres, μ_w	cp	0.2948	n/a
Water Salinity	ppm	10000	n/a

Example 1 &2 Input Data			
Parameter	**unit**	**value**	
Reservoir Properties		**Example 1**	**Example 2**
Reservoir Boundaries:			
Distance to "North" Boundary	ft	5000	5000
Distance to "South" Boundary	ft	5000	5000
Distance to "East" Boundary	ft	5000	5000
Distance to "West" Boundary	ft	5000	5000
Boundary Types (0=Inf, 1=NF, 2= CP)			
Type North Boundary		1	1
Type South Boundary		1	1
Type East Boundary		1	1
Type West Boundary		1	1
Well bore Properties			
Well radius	ft	0.3	0.3
Wellbore Skin, S		0	0
Wellbore Storage Coefficient, C	bbl/psi	0.01	0.01
Constraints			
Max CO_2 Injection rate	MMscf/d	1	2
Max Injection Pressure (Example 1b)	psia	7000	n/a
Duration of Injection	years	10	10
Duration of Subsequent Shut-in	hrs	2500	2500

Table 2—Input Fluid Properties versus Pressure for Example 1 and 2

	CO_2 Properties at 212 F					Water Properties at 212 F			Oil Properties at 212 F (for Example 2)			
Pressure psia	**Z**	**Bg cf/scf**	**cg psi^{-1}**	**ρg g/cc**	**μg cp**	**Bw B/ STB**	**cw psi^{-1}**	**ρw g/cc**	**Bo B/ STB**	**co psi^{-1}**	**ρo g/cc**	**μo cp**
15	1.0060	1.299	0.06822	0.001440	0.01856	1.0426	3.294E-06	0.9665	1.0776	0.03283	0.7431	0.7856
1015	0.8368	0.01566	0.001195	0.119565	0.02014	1.0392	3.225E-06	0.9696	1.1936	0.0006538	0.7033	0.4435
2015	0.6666	0.006280	7.170E-04	0.298041	0.02681	1.0359	3.159E-06	0.9727	1.3434	2.366E-05	0.6593	0.3341
3015	0.5921	0.003728	3.356E-04	0.502084	0.03890	1.0327	3.095E-06	0.9758	1.3179	1.581E-05	0.6721	0.3732
4015	0.6271	0.002965	1.552E-04	0.631247	0.05017	1.0295	3.034E-06	0.9788	1.3000	1.187E-05	0.6813	0.4256
5015	0.6958	0.002634	9.141E-05	0.710700	0.05942	1.0264	2.976E-06	0.9817	1.2863	9.505E-06	0.6886	0.4886
6015	0.7739	0.002442	6.271E-05	0.766399	0.06737	1.0234	2.920E-06	0.9846	1.2752	7.925E-06	0.6946	0.5598
7015	0.8549	0.002313	4.708E-05	0.809090	0.07449	1.0205	2.865E-06	0.9875	1.2659	6.795E-06	0.6997	0.6369
8015	0.9367	0.002219	3.743E-05	0.843722	0.08105	1.0176	2.813E-06	0.9903	1.2579	5.948E-06	0.7041	0.7173
9015	1.0183	0.002144	3.095E-05	0.872902	0.08720	1.0147	2.763E-06	0.9931	1.2508	5.288E-06	0.7081	0.7981
10015	1.0995	0.002084	2.633E-05	0.898158	0.09305	1.0120	2.714E-06	0.9958	1.2446	4.760E-06	0.7116	0.8765

The results for both runs are summarized in Table 3 and Figure 4. The injectivity index, II, and its variation over time is illustrated in Figure 5:

$$II = \frac{q}{p(t) - \overline{p}(t)} \tag{30}$$

Table 3—Results Summary for Examples 1 and 2

Results summary					
		Example 1a	Example 1b	Example 2a	Example 2b
Cumulative Injection	bscf	3.65	1.55	7.31	7.78
Cumulative Injection	mega tonnes	0.190	0.0803	0.379	0.404
Initial Rate	MMscf/d	1.00	1.00	2.00	20
Final Rate	MMscf/d	1.00	0.00	2.00	0
Initial Reservoir Pressure	psia	5000	5000	2000	2000
Final injection pressure	psia	9453	7000	5824	6000
Initial Pore Volume	bbl	53432280	53432280	53432280	53432280
Final Average Pressure	psia	9363.84	7000.42	5706.01	6000
Final Pore Volume	bbl	54136389	53753905	54029657	54079223
Pore Volume Occupied by CO_2	bbl	1380417	638181	3243144	3386849
Injection Efficiency	%	2.583	1.194	6.070	6.339

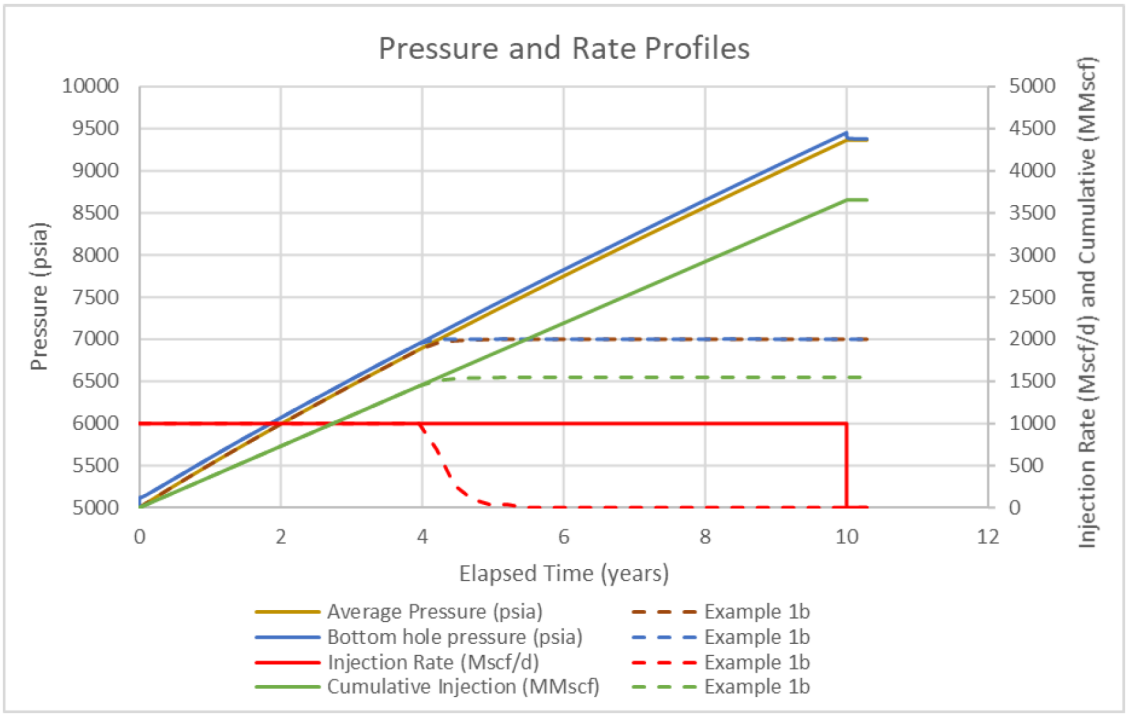

Figure 4—Example 1a and 1b: Injection Profiles

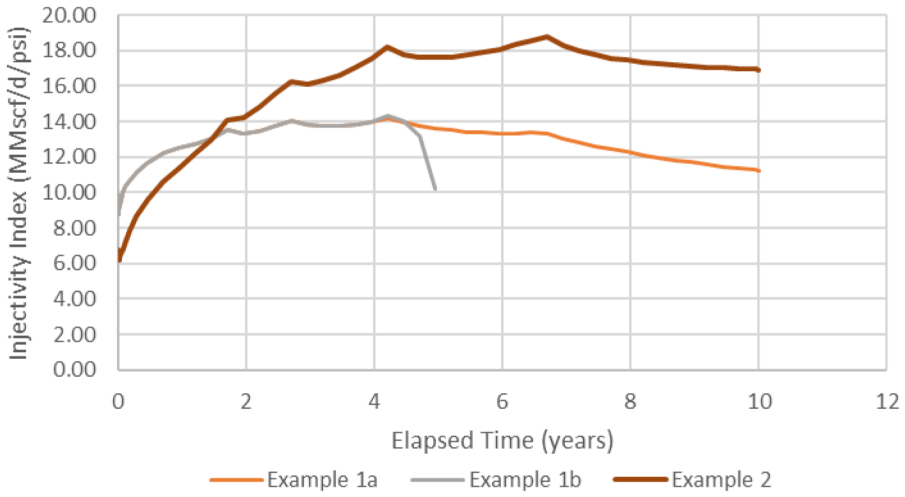

Figure 5—Example 1 and 2: Injectivity Index Variation with Time

The variation is a consequence of the growing gas zone around the well and the increasing pressure, the former tending to improve injectivity because gas mobility is greater than that of water whilst the latter reduces injectivity because the gas viscosity increases with pressure. In this example the injectivity index is high and does not significantly impact the maximum storage of CO_2 or the storage efficiency (the proportion of the total reservoir pore volume occupied by CO_2). Rather, it is the restricted reservoir size and low water compressibility causing the average pressure to rise rapidly which constrains the maximum storage of CO_2 resulting in a very low storage efficiency. In this case it is likely that the maximum storage could be achieved sooner by injecting at a higher rate. The implementation of this method is designed to allow such sensitivity studies.

For Example 1a, the pressure transient response is illustrated on a log-log plot in Figure 6. Pressure change is depicted as continuous lines and the Bourdet derivative is shown dashed. The response during injection is shown in red and is compared with the initial (green) and final (yellow) radial composite model responses. The subsequent build-up response is shown in grey. It is apparent that the injection pressure response is a complex combination of the early and late radial composite responses. This is driven by the radial composite model development over time as illustrated in Figure 7. The fall-off response closely matches the final radial composite response up until the pressure stabilizes and the derivative rolls over. Once the well is shut-in, there is no more propagation of the CO_2 bank and there is no further increase in average pressure and the fall-off reflects the reservoir configuration at the time of the shut-in.

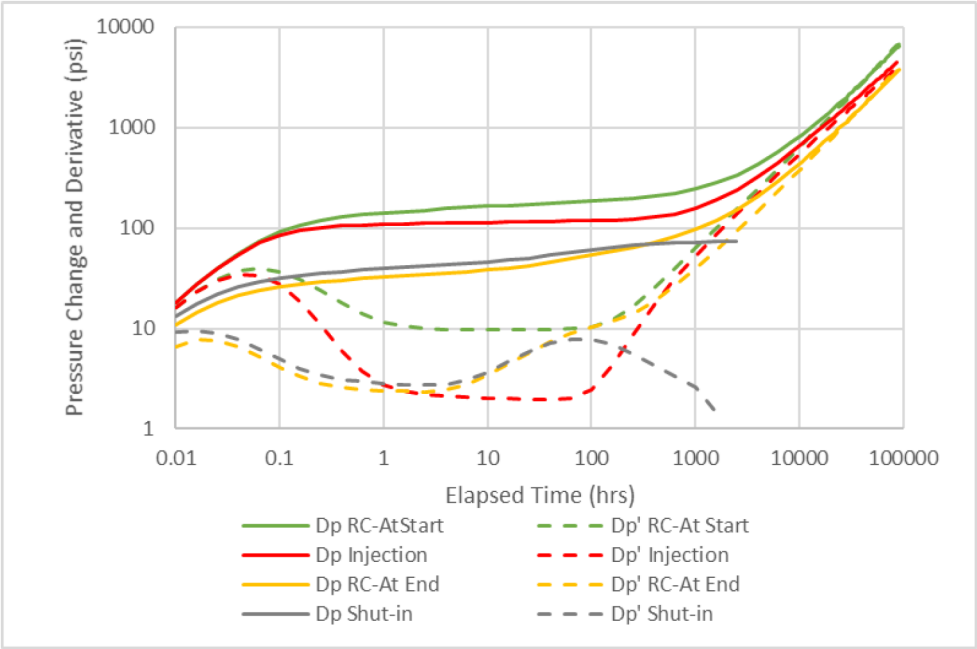

Figure 6—Example 1a: Log-log plot of Pressure Transient Response

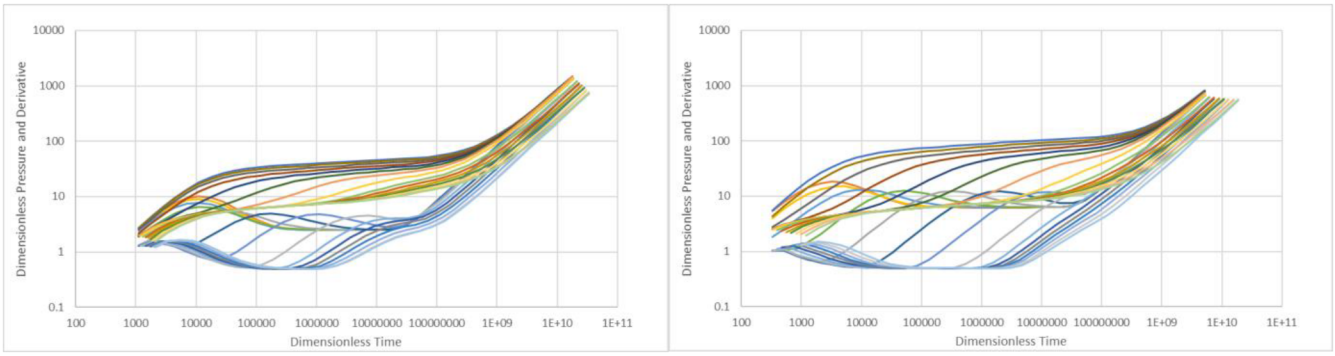

Figure 7—Example 1 (left) and 2 (right): Radial Composite Model Development over Time

Example 2 Oil Reservoir

In this case, the same reservoir as Example 1 is assumed to be full of oil at a static pressure of 2000 psia – a lower pressure assumed to represent a depleted reservoir. Connate water is ignored in this example but in practice should be considered. The oil fluid properties are listed in Table 2. CO_2 is injected at 2 MMscf/d (0.0379 Mt/year) and the results following ten years of injection are given in Table 3; a comparison of the injectivity index with Example 1 is shown in Figure 5 and the development over time of the radial composite model in Figure 7. In comparison to Example 1, the injection efficiency is improved mainly due to the lower compressibility of oil compared to water but also thanks to the lower reservoir pressure and improved injectivity index. A second case (Example 2b) with a maximum injection rate of 20 MMscf/d (0.379 Mt/year) and a maximum pressure constraint of 6000 psia demonstrates how in this case, the maximum CO_2 storage can be reached in two years rather than ten as illustrated in Figure 8

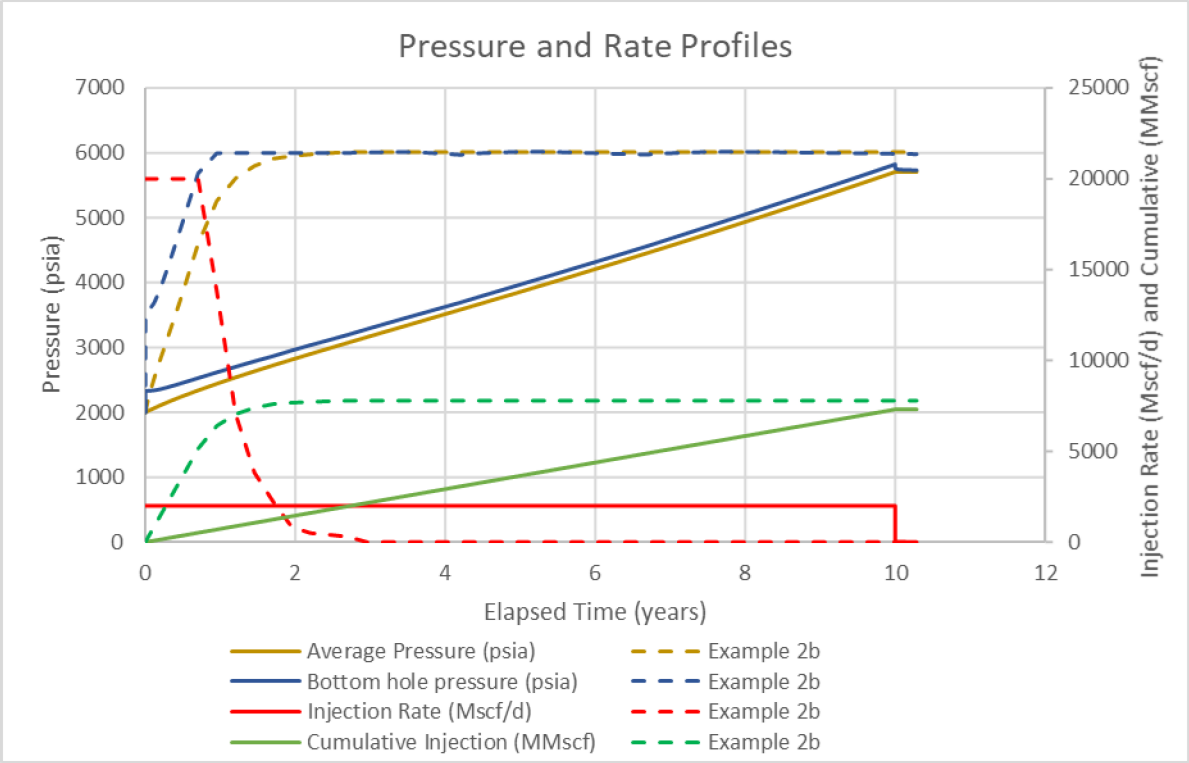

Figure 8—Example 2 and 2b: Injection Profiles

Comparison with Numerical Models

A commercial numerical reservoir simulator was used to model the same scenario as Example 1. The simulator included gravity and solubility. Logarithmically spaced radial grids around the well were defined to model the early time response. A comparison of the predicted injection pressure compared to the semi-analytical method described in this study is shown in Figure 9. The pressure change is virtually the same, but the derivative is noisy which is often the case with numerical models when an advancing fluid bank crosses grid boundaries. A second numerical run was made with ten layers to better simulate the effects of gravity. The saturation profile was clearly distorted compared to the simple piston-like displacement assumption of the semi-analytical method but there was no impact on the predicted wellbore pressure. This suggests that pressure transients are not sensitive to the geometry of an advancing flood front.

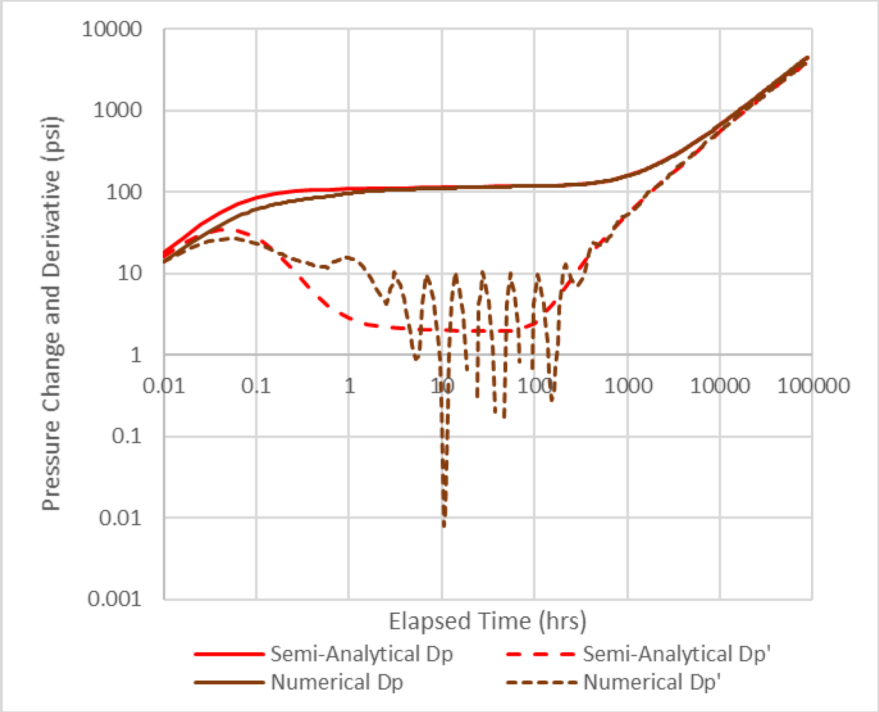

Figure 9—Example 1: Comparison with a Numerical Simulator

It was also noted that the numerical model was surprisingly insensitive to the solubility of CO_2 in water. It has yet to be confirmed whether this behaviour is a limitation in the simulator rather than a physical effect.

It was not possible to simulate the injection of CO_2 into an oil reservoir with the available black oil simulator and consequently the results of Example 2 have not been compared.

Conclusions

A semi-analytical model appears to adequately predict CO_2 injectivity into saline aquifers and depleted hydrocarbon reservoirs. The model requires minimal input which makes it useful for general CO2 storage screening scoping studies. It includes neither gravity nor solubility but that does not appear to impair the accuracy of its prediction. However, it does not predict the long-term distribution of CO_2 in the reservoir which would be an important factor in long term monitoring requiring detailed studies for which numerical simulation models with more detailed physics are required.

Within the petroleum industry, there may be a need for improvement in some commercial software packages to better accommodate the injection of CO_2 particularly in black oil numerical simulators where currently it is not possible to distinguish between hydrocarbon gas in the reservoir and injected CO_2 and only a fully compositional simulator is likely to adequately model the full physics of the problem when the CO_2 becomes supercritical. It should be possible to implement the semi-analytical method described in this paper into standard well test analysis software to facilitate its use.

The semi-analytical model is based on a two-zone radial composite analytical solution whose parameters vary with time. It is possible that a three-zone radial composite model might better model the two-phase region in between the fully saturated CO_2 gas zone around the well and the undisturbed reservoir fluids further away. But based on the reported numerical studies, it seems unlikely that it would result in any significant change in the prediction of well pressures.

Changes in temperature have not been considered in this study and the impact of injecting cold CO2 into the reservoir may need to be taken into account dependent on how much the fluid properties are likely to change as a result.

It is recommended that prior to the injection of CO_2 into a well, it is first tested either in production or injection of the existing reservoir fluids and then shut-in for either a build-up or fall-off. The resulting pressure transient would enable a better reservoir description – particularly the permeability and influence of nearby boundaries.

This study confirms that injecting CO_2 into closed saline aquifers is limited by either the maximum pressure that the formation can endure before fracturing and potentially leaking through the cap rock or the working pressure of the injection pumps. As already observed by Ehlig-Economides & Economides (2009), in either case and mainly because of the low compressibility of water, the maximum volume occupied by the CO_2 in such reservoirs will be a small proportion of the total pore volume. In depleted oil reservoirs particularly those with a gas cap or indeed depleted gas reservoirs, the reservoir fluid compressibility is at least an order of magnitude higher resulting in increased CO2 storage as a function of reservoir pore volume. CO_2 injection into reservoirs connected to mobile aquifers can potentially provide the highest injection efficiency, there being no increase in average pressure as the reservoir fluids are displaced. However, in such cases, it will be even more important to study how the CO_2 might migrate over time.

Nomenclature

A	reservoir area (m^2)
A_p	dimensionless reservoir area
A'_D	dimensionless reservoir area
A_1	inner zone area (m^2)
A_2	outer zone area (m^2)
B	formation volume factor
B_g	gas formation volume factor
C	wellbore storage coefficient (m^3/Pa^{-1})
C_p	dimensionless wellbore storage coefficient
c_f	rock compressibility (Pa^{-1})
c_g	gas compressibility (Pa^{-1})
c_o	oil compressibility (Pa^{-1})
c_t	total compressibility (Pa^{-1})
c_w	water compressibility (Pa^{-1})
h	reservoir thickness (m)
II	Injectivity Index ($m3/s/Pa$)
k	permeability (m^2)
p	bottomhole pressure (Pa)
$\overline{p}$	average reservoir pressure (Pa)
p_D	dimensionless pressure
p_i	initial (static) reservoir pressure (Pa)
PM	Pressure Match (Pa^{-1})
q	flow rate (m^3/s)
r_1	radial composite zone 1 radius (m)
r_{1D}	dimensionless radial composite zone 1 radius
r_w	wellbore radius (m)
S	Wellbore Skin factor
S_g	gas saturation
S_o	oil saturation
S_w	water saturation

S_{wi} irreducible water saturation
t time (s)
t_p dimensionless time
TM Pressure Match (s_{-1})
V_g Gas volume (m_3)
V_w Water volume (m_3)
X_e width of rectangular reservoir (x direction) (m)
Y_e breadth of rectangular reservoir (y direction) (m)
X_w distance of well from reservoir origin in x direction (m)
Y_w distance of well from reservoir origin in y direction (m)
ϕ porosity
μ viscosity ($Pa\ s$)
κ mobility thickness ratio
ω storativity ratio

References

1. Agarwal, Ram G., Al-Hussainy, Rafi, and H.J. Ramey. 1970: "An Investigation of Wellbore Storage and Skin Effect in Unsteady Liquid Flow: I. Analytical Treatment." *SPE J.* **10** (1970): 279–290. doi: https://doi.org/10.2118/2466-PA
2. Bourdet, D., Whittle, T.M., Douglas, A.A., Pirard, V.M. 1983: "A New Set of Type Curves Simplifies Well Test Analysis", *World Oil*, May 1983.
3. Bourdet, Dominique, Ayoub, J.A., and Y.M. Plrard. "Use of Pressure Derivative in Well-Test Interpretation." *SPE Form Eval* **4** (1989): 293–302. doi: https://doi.org/10.2118/12777-PA
4. Christine Ehlig-Economides, Michael J. Economides. 2010: "Sequestering carbon dioxide in a closed underground volume", *Journal of Petroleum Science and Engineering*, Volume **70**, Issues 1–2, Jan 2010, Pages 123-130, ISSN 0920-4105. doi: https://doi.org/10.1016/j.petrol.2009.11.002.
5. Gringarten, Alain C., and Henry J. Ramey. 1973: "The Use of Source and Green's Functions in Solving Unsteady-Flow Problems in Reservoirs." *SPE J.* **13** (1973): 285–296. doi: https://doi.org/10.2118/3818-PA
6. Kamal, Medhat M., Tian, Chuan, and Fnu Suleen. "Pressure Transient Analysis of Polymer Flooding With Coexistence of Non-Newtonian and Newtonian Fluids." *SPE Res Eval & Eng* **22** (2019): 1172–1184. doi: https://doi.org/10.2118/181473-PA
7. Kikani, Jitendra, and Gardner W. Walkup. 1991: "Analysis of Pressure-Transient Tests for Composite Naturally Fractured Reservoirs." *SPE Formation Evaluation* June (1991): 176–182. doi: https://doi.org/10.2118/19786-PA
8. David H.-S Law and Stefan Bachu. 1996: "Hydrogeological and Numerical Analysis of Co2 Disposal in Deep Aquifers in the Alberta Sedimentary Basin", *Energy Conversion and Management*, Volume **37**, Issues 6–8, Pages 1167–1174, ISSN 0196-8904. doi: https://doi.org/10.1016/0196-8904(95)00315-0.
9. Mathias, S.A., González Martínez de Miguel, G.J., Thatcher, K.E. Zimmerman, R.A. 2011: "Pressure Buildup During CO2 Injection into a Closed Brine Aquifer". *Transp Porous Med* **89**, 383–397 (2011). doi: https://doi.org/10.1007/s11242-011-9776-z
10. McMillan Burton, Navanit Kumar, and Steven L. Bryant. 2008 "Time-Dependent Injectivity During CO2 Storage in Aquifers" paper SPE-113937-MS presented at the SPE/DOE Improved

Oil Recovery Symposium held in Tulsa, Oklahoma, U.S.A., 19–23 April 2008. doi: https://doi.org/10.2118/113937-MS

11. Nordbotten, J.M., Celia, M.A. & Bachu, S. 2005: "Injection and Storage of CO2 in Deep Saline Aquifers: Analytical Solution for CO2 Plume Evolution During Injection." *Transp Porous Med* **58**, 339–360. doi: https://doi.org/10.1007/s11242-004-0670-9
12. Yannick Peysson, Laurent André, Mohamed Azaroual, 2014: "Well injectivity during CO2 storage operations in deep saline aquifers—Part 1: Experimental investigation of drying effects, salt precipitation and capillary forces", *International Journal of Greenhouse Gas Control*, Volume **22**, 2014, Pages 291–300, ISSN 1750-5836. doi: https://doi.org/10.1016/j.ijggc.2013.10.031.
13. Ringrose, P.S., Meckel, T.A. 2019: "Maturing global CO2 storage resources on offshore continental margins to achieve 2DS emissions reductions". *Sci Rep* **9**, 17944 (2019). doi:10.1038/s41598-019-54363-z
14. Stehfest, H. 1970: "Algorithm 368, Numerical Inversion of Laplace Transform," *D-5 Communication of the ACM* (Jan, 1970) **13**, No. 1, 47–49. doi: https://doi.org/10.1145/361953.361969